Available online at www.sciencedirect.com
ScienceDirect
Journal of Power Sources 172 (2007) 346–357
JOURNAL OF POWER SOURCES
www.elsevier.com/locate/jpowsour

Diffusive resistance analysis in fuel cells Part 2. Some methods and examples

Paolo Costa, Barbara Bosio *

Dipartimento di Ingegneria delle Costruzioni, dell'Ambiente e del Territorio, Università degli Studi di Genova, Via Opera Pia 15, 16145 Genova, Italy

Received 8 December 2006; received in revised form 23 April 2007; accepted 29 April 2007
Available online 5 May 2007

Abstract

In the first part of this work a rationalisation and a generalisation of the approach to the analysis of the diffusive resistances in laboratory-scale fuel cells and electrodes was recommended and some interpretation tools for the purpose were suggested and some simple reference cases discussed.

This second part is mainly devoted to some applications to experimental data. In particular, some sets of experimental data from Ansaldo Fuel Cells laboratories are examined. The data regard molten carbonate fuel cells at a 10 cm × 10 cm laboratory scale; a first set of data was obtained under constant current and changing utilisation factor conditions; the second under limit current conditions.

The analysis indicated that the cathodic diffusive resistances are not important and the anodic ones, when correctly determined, do not depend on the anodic gas flow rate, but are likely to be localised in the liquid phase.

Keywords: Fuel cells; Transport phenomena; Diffusion resistance; Experimental data

1. Introduction

Many fuel cell systems at the laboratory scale are large enough to require a more detailed analysis. Often, while the uniform temperature and voltage assumptions can be considered appropriate, the uniform concentration assumption may correspond to a gross over simplification. The analysis of a set of laboratory data obtained from systems of this kind requires interpretation instruments of an intermediate level, which, on the one hand, overcome the simple electrode concept and, on the other hand, avoid the cumbersome and time-consuming structure of detailed large-scale models.

In the first part of this work [1] some principal concepts were presented and these can be summarised as follows:

- The local electrochemical kinetics of a finite electrode can be expressed in terms of an external, constant reference condition that yields a local kinetic expression that is often a function of a unique variable, for instance, the concentration or the utilisation degree of a key component of the fluid phase.
- Given local kinetics of this kind, for instance, a linear irreversible one

$$j = j_{*\mathrm{o}} \left(\frac{C_\mathrm{A}}{C_\mathrm{Ao}} \right) \left(1 - \frac{j}{j_\mathrm{L}} \right) \exp(\beta \eta_\mathrm{o}) \tag{1}$$

the statements

$$k_\mathrm{o} = \left(\frac{j_{*\mathrm{o}}}{nFC_\mathrm{Ao}} \right) \exp(\beta \eta_\mathrm{o}) \tag{2}$$

$$r = \frac{j}{nF} = k_\mathrm{o} C_\mathrm{As} = k_\mathrm{c}(C_\mathrm{A} - C_\mathrm{As}) = KC_\mathrm{A} \tag{3}$$

$$K = \left(\frac{1}{k_\mathrm{o}} + \frac{1}{k_\mathrm{c}} \right)^{-1} \tag{4}$$

make it possible to reduce the electrochemical kinetics to the classical formulation of a first-order heterogeneous reaction at the boundary.
- When the local kinetics is averaged on the surface of a finite electrode, the effect of the concentration field can be taken into account by the coefficient

$$\frac{1}{A} = \frac{C_\mathrm{Am}}{C_\mathrm{Ao}} = \left(\frac{\int_S C_\mathrm{A}\, \mathrm{d}S}{C_\mathrm{Ao} S} \right), \quad A > 1 \tag{5}$$

* Corresponding author.
E-mail address: bosio@diam.unige.it (B. Bosio).

0378-7753/$ – see front matter © 2007 Elsevier B.V. All rights reserved.
doi:10.1016/j.jpowsour.2007.04.063

Nomenclature

A	corrective coefficient, from the averaging operation
c_o	asymptotic (low current) corrective coefficient; see Eq. (B5) in Part 1
C	see Eq. (19)
C_i	volumetric concentration of the component i [kmol m^{-3}]
D_A	diffusivity [m^2 s^{-1}]
F	molar flow rate [mol s^{-1}]
j	current density [A m^{-2}]
J	mean electrode current density [A m^{-2}]
k_a	apparent kinetic constant [m s^{-1}]
k_c	mass transfer coefficient [m s^{-1}]
k_f	flow dynamic coefficient [m s^{-1}]
k_o	intrinsic kinetic constant [m s^{-1}]
K	global kinetic constant, local value [m s^{-1}]
L	length [m]
m	gas–liquid partition coefficient
M	molecular weight [kg mol^{-1}]
n	stoichiometric coefficient for electrons, absolute value
n_i	stoichiometric coefficients
N	molar flux [mol m^{-2} s^{-1}]
P	absolute pressure [N m^{-2}]
Pe	Peclet number
q	volumetric flow rate [m^3 s^{-1}]
r	reaction rate, per unit surface [kmol m^{-2} s^{-1}]
r_L	limit reaction rate [kmol m^{-2} s^{-1}]
r_m	mean reaction rate [kmol m^{-2} s^{-1}]
R	gas constant [J kmol^{-1} K^{-1}]
Re	Reynolds number
s	diffusive equivalent thickness [m]
S	electrode surface [m^2]
Sc	Schmidt number
Sh	Sherwood number
T	absolute temperature [K]
u	utilisation factor
v	velocity [m s^{-1}]
V	voltage [W A^{-1}]
x	advancement degree [kmol m^{-3}]
X	see Eq. (19)
y_A	mol fraction of the key reagent
Y	see Eq. (19)

Greek letters

α	reaction order
β	symmetry factor
γ	apparent reaction order
η	adimensional potential loss
μ	dynamic viscosity [kg m^{-1} s^{-1}]
ν	mol number variation in respect to the key
ν_i	stoichiometric coefficient
ρ	density [kg m^{-3}]
ζ	adimensional axial coordinate

Subscripts and superscripts

an	anode
A	key reagent (hydrogen at the anode, oxygen at the cathode)
c	concentration
ca	cathode
cp	central point
CP	condensed phases
eq	equilibrium
G	gas phase
i	generic component
L	limit
LP	liquid phase
m	mean value
M	maximum value
o	inlet
r	reference
s	electrode surface
T	total
*	exchange
′	refers to the other electrode

so that, for linear kinetics, the apparent constant k_a and the limit constant k_L

$$k_a = \frac{r_m}{C_{Ao}} = \frac{K}{A}, \qquad k_L = \frac{r_L}{C_{Ao}} = \frac{k_c}{A_L} \tag{6}$$

do not coincide with the global constant K and the transport coefficient k_c, respectively, and their relationship with the intrinsic reaction constant k_o

$$\frac{1}{Ak_a} = \frac{1}{k_o} + \frac{1}{A_L k_L} \tag{7}$$

becomes more complex.

- In particular, the coefficients A and A_L also depend on a flow dynamic constant, the fluid flow rate per unit electrode surface

$$k_f = \frac{q}{S} \tag{8}$$

that is the maximum apparent constant compatible with the reagent availability.

- The behaviour of the electrode can be directly interpreted in terms of Eq. (4) only if it is "simple", that is subject to a uniform composition field. Otherwise, what is observed is the result of at least two factors: the local diffusive resistances set and the concentration distribution on the electrode. The first effect can be properly determined only after estimating the second with an adequate physical–mathematical description.
- In many cases a description of sufficient complexity can be obtained by using the classical instruments of the chemical reactor theory. Appendices D and E are devoted to some relevant results of this approach.

2. Analysis and correlation methods

The characterisation of a fluid flow electrode or cell usually consists of the measurement of the current–voltage characteristic curves. Each of these curves is obtained by keeping the cell geometry and the inlet fluid composition and flow rate constant.

2.1. Constant flow analysis

In most cases, the flow dynamic coefficient k_f is known and constant, while the apparent constant (k_a, that is the current) and the intrinsic constant (k_o, that is the voltage), as well as the limit constant (k_L, that is the limit current) need to be measured. In the case of a simple electrode the problem ends here, but it is often advisable to carry the investigation a little further.

In fact, in the first place, Eq. (4) may be inadequate to describe complex electrodes, in terms of geometry, flow pattern or, particularly, non-uniform composition fields. In the second place, Eq. (4) is certainly wrong when the reagent availability begins to manifest its limiting effects (low k_f, that is high utilisation factors). In the third place, also for low utilisations, Eq. (4) and its asymptotic solution may not be fully adequate and require the introduction of a corrective coefficient c_o different from unity (see Part 1, Appendix B).

When Eq. (4) is doubtful, the reference to a formulation with a wider range of validity, such as Eq. (7), is useful. The differences between Eqs. (4) and (7) are often appreciable, even in the low current range, where the local linearisation in Eqs. (5) and (6) of Part 1 can be transformed in terms of mean density current

$$\eta_o \approx \left(\frac{1}{\beta}\right)\left[\ln\left(\frac{J}{J_{*o}}\right) + \frac{c_o J}{J_L}\right] \tag{9}$$

$$\eta_{oc} \approx \frac{c_o J}{\beta J_L} = \frac{c_o k_a}{\beta k_L} \tag{10}$$

by allowing for the asymptotic correction c_o at low current. In such a way, the concentration polarisation η_c is still considered proportional to the mean current density J and inversely proportional to the limit value J_L of the mean current density (that is proportional to the ratio k_a/k_L between the apparent and the limit constant), but the proportionality coefficient is determined as c_o/β and only a careful examination of the characteristic curve can suggest whether it is correct or not to assume a unitary value for the asymptotic constant c_o and, in that case, how the correct value differs from unity for the constant. Obviously, when the analysis of the concentration polarisations is made in terms of ratios, all this discussion can be avoided, but it is important to have a correct estimation of the absolute values of polarisation. In particular, if the experimental value of the ratio J/η_{oc} is identified with βJ_L, this leads to an overestimation of the limit current; on the other hand, if the polarisation is estimated from an independent measurement of the limit current, such as $\eta_{oc} = J/\beta J_L$, this leads to its underestimation.

Finally, once a correct value for k_L is determined, the local transport coefficient k_c can be determined in its turn only by correcting k_L by means of a coefficient A_L, usually different from (greater than) unity.

2.2. The effects of the flow conditions

In all cases, the structure of the limit constant k_L or, better, the transfer coefficient k_c and the effects of the flow conditions on them is to be carefully examined, even if Eq. (4) stands. This can be done in an empirical way, by correlating experimental data on the limit current at different flow rates or different inlet compositions in terms of adimensional coefficients, for instance, by expressing the Sherwood number, containing k_L or k_c, as a function of the Reynolds and Schmidt numbers, or their product, the Peclet number; alternatively, with a theoretic approach to be subjected to an empirical confirmation, such correlations can be derived from a physical–mathematical description. For instance, in Part 1, Appendix C, Eq. (C19) for the uniform velocity electrode is equivalent to the correlation

$$Sh = 1.128\, Re^{1/2}\, Sc^{1/2} = 1.128\, Pe^{1/2} \tag{11}$$

$$Sh = \frac{k_L L}{D_A}, \qquad Re = \frac{\rho v L}{\mu},$$
$$Sc = \frac{\mu}{D_A \rho}, \qquad Pe = \frac{vL}{D_A} \tag{12}$$

2.3. Constant current analysis

When the object of the analysis is more particularly focused on mass transfer resistances and their dependence on the flow conditions, the desired information can be more quickly and simply obtained by varying the inlet conditions. For instance, the measurements can be performed under the constant current restraint and by changing the velocity at the electrode through flow rate changes, so that the current density J becomes a constant, while the limit current J_L is a variable.

For the identification of the diffusive resistances from voltage measurements at constant current the linearisation of Eqs. (9) and (10) can be used [2], but it is often preferable to make a direct reference to the non-linear form of Eq. (7), allowing for a constant k_a. However, it should be remembered that, for a complex electrode, k_L does not coincide with k_c and, moreover, for measurements under different flow rates, the reference condition for the limit current is not evident or obvious. On the contrary, it is often preferable to choose another type if reference condition, i.e. a very high flow rate condition (that is a very low utilisation factor), at which the transport resistances connected to flow dynamics become very low or even completely negligible.

As usual, any refinement of the analysis passes through a more detailed description of the flow and composition fields along the electrode, that is the reliable calculation of the coefficients A and A_L. Making reference to working conditions with constant current and changing utilisation factor, in Eq. (7) k_a is a constant while k_L and $k_c = K_L A_L$ are variables, depending on k_f. It is then preferable to write Eq. (7) as follows:

$$\frac{1}{k_o} = \frac{1}{A k_a} - \frac{1}{k_c} = \frac{1}{k_a} - \frac{1}{k_c} - \left(\frac{(A-1)/A}{k_a}\right) \tag{13}$$

As already said, under these conditions it is not particularly useful to make reference to low currents, with k_o controlling

or high currents, with $k_L = k_c/A_L$ controlling, but it is better to refer to particularly favourable flow conditions (high flow rates, the current remaining unchanged), in which the transport coefficient is high. Moreover, at high flow rates, the utilisation factor approaches zero and the averaging coefficient A approaches unity, while k_c increases and $1/k_c$ decreases as far as, in some cases, to become negligible. Under these reference conditions Eq. (13) attains its limit form

$$\frac{1}{k_{or}} = \frac{1}{k_a} - \frac{1}{k_{cM}} \tag{14}$$

and, by combining Eqs. (13) and (14), a useful identification tool is obtained

$$\frac{k_{or}}{k_o} = \frac{1 - (k_a/k_c) - ((A-1)/A)}{1 - (k_a/k_{cM})} = \exp(-\beta\eta_r), \quad \text{with } \eta_r = V - V_r \tag{15}$$

by means of which the voltage loss is expressed, with respect to the reference, in terms of transport coefficients.

Starting with polarisation data, Eq. (15) can be used in order to obtain the transport coefficient and its dependence on the inlet flow rate, on condition that an acceptable theoretical evaluation of the averaging coefficient A can be performed; inversely, Eq. (15) can be used to obtain information on the composition field starting with some kind of estimation of the transport coefficient. In the first section an example of the first type of approach will be discussed.

Here a comment on small perturbations should be added: when the inlet flow rate is only slightly changed, Eq. (15) can be written in the simple differential form

$$\beta\, d\eta_r \approx -\left(\frac{k_a}{k_c}\right) d\ln(k_c) \tag{16}$$

on condition that $k_a \ll k_c$ and, coherently, $A \approx 1$. In all the other cases it is probably better to make a direct reference to the finite formulation of Eq. (15).

So, two difficulties can be underlined in using perturbative measurements; first of all they must be performed in terms of variations large enough to induce well measurable voltage effects in all instances; moreover, they are not always directly interpretable by neglecting the effects of the composition fields (A different from unity and depending on the flow rate). On the contrary, under the opposite condition, where the transport coefficient depends slightly on the flow rate (see the following section), the potential change is mainly due to differences in the flow field

$$\beta\, d\eta_r \approx d\ln(A) \tag{17}$$

and the evaluation of k_c cannot be considered unrelated to an estimation of A.

2.4. Analysis in terms of limit currents

For each limit current condition, direct k_L measurements lead univocally to the transport coefficient k_c, on condition that the effect of the composition field, according to the second equation in (6), is taken into account through the coefficient A_L. Limit current data are particularly suitable because the estimation of A_L is often simpler than that of the generic coefficient A, which is also a function of the ratio between the actual and the limit current. On the other hand, each characteristic curve gives one limit current value only, so that these data are relatively rare.

However, it is worth underlining once more that the diffusive resistance cannot be automatically and directly determined from the limit current alone.

3. An example of constant current analysis

In Tables 1–3 and Fig. 1, some series of experimental data on an Ansaldo Fuel Cells molten carbonate fuel cell are reported.

The experimental work was conducted at the Ansaldo laboratories; the experimental apparatus and test procedure have been described elsewhere [3]. Here two test series with a perturbative nature are specifically discussed: for each series, in Tables 1 and 2, respectively, a central point is defined and the working range is reported in terms of different inlet flow rates, while the cell current is maintained rigorously constant at the central point value. The cell temperature and the humidification conditions are also maintained unchanged. Each series is articulated in two subseries and in each subseries the inlet flow rate to one electrode is varied while the flow rate to the other electrode is constant. Each experimental point refers to the stationary con-

Table 1
Ansaldo Fuel Cells: series I—test conditions

Central point	
Anodic flow rates [N m^3 h^{-1} × 10^3] (y_{Ao} = 0.225, A = H_2)	
H_2	7.43
CO_2	2.24
N_2	20.50
H_2O	2.86
Total	33.03
Cathodic flow rates [N m^3 h^{-1} × 10^3] (y_{Ao} = 0.161, A = O_2)	
Air	84.66
CO_2	14.31
N_2	6.23
Total	105.20
Cell dimensions (cm^2)	10 × 10
Cell current (A)	5.5
Cell voltage (V)	0.814
Anode	
H_2 utilisation (%)	30.97
Cathode	
CO_2 utilisation (%)	16.08
O_2 utilisation (%)	6.79
Anodic tests	
Anodic flow rates	$0.5q_{an\,cp} < q_{an} < 1.5q_{an\,cp}$
Cathodic flow rates	$q_{ca} = q_{ca\,cp}$ = const.
Cathodic tests	
Anodic flow rates	$q_{an} = q_{an\,cp}$ = const.
Cathodic flow rates	$0.5q_{ca\,cp} < q_{ca} < 1.5q_{ca\,cp}$

Table 2
Ansaldo Fuel Cells: series II—test conditions

Central point	
Anodic flow rates [$N\,m^3\,h^{-1} \times 10^3$] ($y_{Ao} = 0.727$, A = H_2)	
H_2	7.80
CO_2	2.00
N_2	0.00
H_2O	0.93
Total	10.73
Cathodic flow rates [$N\,m^3\,h^{-1} \times 10^3$] ($y_{Ao} = 0.129$, A = O_2)	
Air	91.50
CO_2	8.00
N_2	46.50
Total	146.00
Cell dimensions (cm^2)	10 × 10
Cell current (A)	5.5
Cell voltage (V)	0.768
Anode	
H_2 utilisation (%)	29.50
Cathode	
CO_2 utilisation (%)	28.77
O_2 utilisation (%)	6.11
Anodic tests	
Anodic flow rates	$0.5q_{an\,cp} < q_{an} < 1.5q_{an\,cp}$
Cathodic flow rates	$q_{ca} = q_{ca\,cp}$ = const.
Cathodic tests	
Anodic flow rates	$q_{an} = q_{an\,cp}$ = const.
Cathodic flow rates	$0.5q_{ca\,cp} < q_{ca} < 1.5q_{ca\,cp}$

Table 3
Ansaldo Fuel Cells: series I and II—anodic results

u_{H_2}	X[a]	X'[b]	V [mV]	Y[c]
Series I, anodic—$y_{Ao} = 0.225$				
0.2010	0.250	0.209	828	0.735
0.2382	0.297	0.249	825	0.708
0.2817	0.352	0.297	818	0.648
0.3097	**0.388**	**0.329**	**814**	**0.617**
0.3440	0.433	0.368	809	0.579
0.4425	0.564	0.485	785	0.429
0.6186	0.812	0.716	723	0.198
u_{H_2}	X[a]	X'[b]	V [mV][d]	Y[c]
Series II, anodic—$y_{Ao} = 0.727$				
0.1967	0.328	0.204	789	0.698
0.2269	0.376	0.237	783	0.648
0.2682	0.442	0.282	773	0.571
0.2950	**0.484**	**0.312**	**768**	**0.536**
0.3278	0.535	0.349	759	0.479
0.4215	0.680	0.460	729	0.330
0.5901	0.938	0.677	645	0.116

The bold data are related to the "central point" of the Series.
[a] $X = 2(A-1)/A$; $A = -y_{Ao} - [(1+y_{Ao})/u]\ln(1-u)$.
[b] $X' = 2(A'-1)/A'$; $A' = -(1/u)\ln(1-u)$.
[c] $Y = \exp[-\beta(\eta - \eta_r)]$. The assumption $\beta = 1/2$ is made and the reference potential is defined so that $\eta = 0$ for $A = 1$.
[d] The choice of a unique external reference for both series I and II requires that the voltage data of series II are corrected by adding 34 mV, allowing for the Nernst concentration effect.

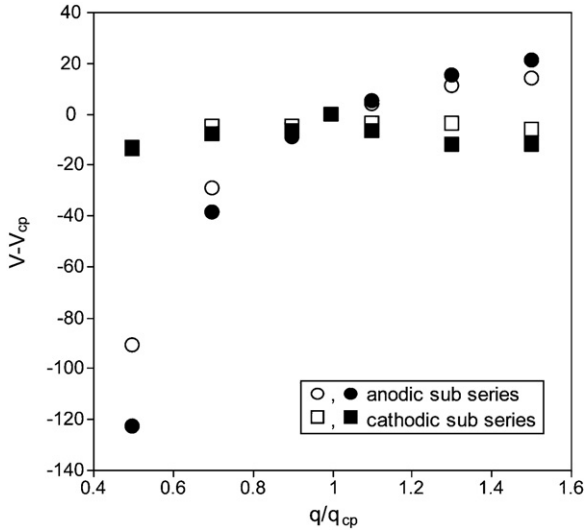

Fig. 1. Rough experimental results: voltage–flow rate trend for the four sub-series. *x*-Axis: ratios of the actual flow rate and the proper central point one; *y*-axis: differences between the actual cell voltage and the proper central point one.

dition attained after each flow rate change. The results, in terms of cell voltage as a function of the inlet flow rate, are reported in Tables 3 and 4 and are shown as a whole in Fig. 1.

3.1. Anodic tests

The figure shows immediately that the cell is much more sensitive to the anodic flow rate changes; this is the reason why the analysis will be focused on the behaviour of the anode.

An a priori evaluation of the order of magnitude of the diffusive resistances of the MCFCs built by Ansaldo Fuel Cells, and in particular the evaluation of the anodic resistances, has suggested that they are mainly localised in the condensed or still phases and, then, independent of flow dynamics (independent of the flow rate and the utilisation factor): resistances of this kind, independent of the flow pattern along the electrode, can be localised in the plate holes, the catalyst layer, and the liquid electrolyte.

Table 4
Ansaldo Fuel Cells: series I and II—cathodic results

Series I, cathodic		Series II, cathodic	
u_{CO_2}	V [mV]	u_{CO_2}	V [mV][a]
0.1072	808	0.1918	756
0.1237	810	0.2213	756
0.1462	810	0.2616	761
0.1608	**814**	**0.2877**	**768**
0.1787	809	0.3196	761
0.2297	809	0.4109	760
0.3214	801	0.5753	754

The bold data are related to the "central point" of the Series.
[a] The choice of a unique external reference for both series I and II requires that the voltage data of series II are corrected by adding 34 mV, allowing for the Nernst concentration effect.

By comparison, the resistances inside the homogeneous moving gas phase appear to be less important. So, in a first approximation, confirmed by Eq. (15), the assumption

$$k_c = k_{cM} = \text{const.} \tag{18}$$

can be introduced and the correlation

$$Y = 1 - CX, \quad Y = \exp(-\beta\eta_r), \quad X = 2\left[\frac{A-1}{A}\right],$$

$$C = \frac{k_c}{2(k_c - k_a)} \tag{19}$$

is obtained.

In such a way, the first equation in (19) foresees a linear relationship between the voltage variable Y and the composition variable X, the linearity constant C being directly connected to the transport coefficient.

The coefficient A and, then, the variable X assumes a specific value at each experimental point, depending on the concentration distribution along the anodic side of the cell, especially for the hydrogen concentrations. These values are not easily accessible: a first attempt at a rough estimation should lead to assume the arithmetic mean $C_{Am} \approx C_{Ao}(1 - (u/2))$, to which $A \approx 1 + (u/2)$ and $X \approx u$ correspond; nevertheless, this first approximation is sufficiently correct only for very low utilisation factors. Fig. 2 demonstrates that the identification of X with u does not allow a satisfying correlation of the experimental data.

Now, if the single adduction channel of the cell is schematised as an ideal tubular reactor with an irreversible first-order reaction (see Part 1, Appendix C2 and Part 2, Appendix D) and, instead of the uniform flow rate assumption, the flow rate changes that are due to the hydrogen consumption ($\nu = 1$) along the axial coordinate are explicitly taken into account (see Appendix E2), a reasonable estimation of the averaging coefficient A is

$$A = -y_{Ao} - \left[\frac{1 + y_{Ao}}{u}\right] \ln(1 - u) \tag{20}$$

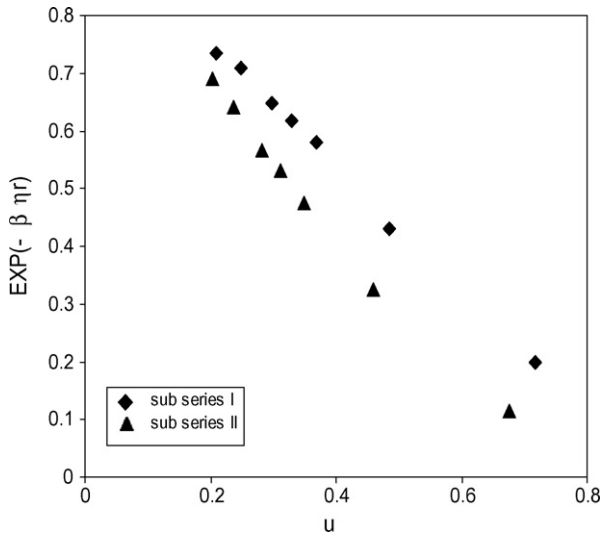

Fig. 2. The anodic polarisation as a function of the utilisation factor.

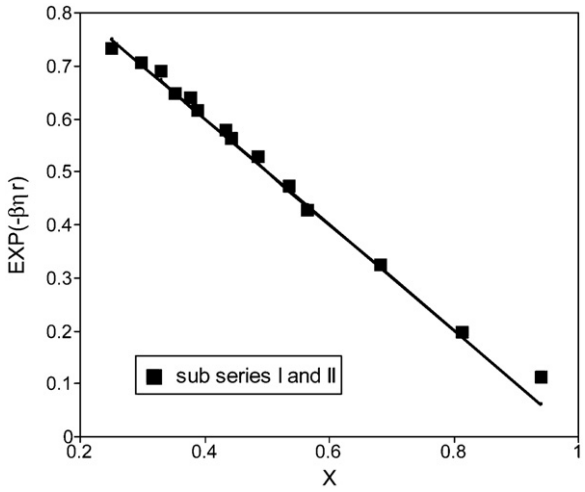

Fig. 3. The anodic polarisation as a function of the variable $X = 2[(A-1)/A]$ with $A = -y_{Ao} - [(1 + y_{Ao})/u] \ln(1 - u)$.

and only when both y_{Ao} and u are very low can the variable X of Eq. (19) be confused with u:

$$y_{Ao} \to 0, \quad u \to 0, \quad A \approx 1 + \frac{u}{2}, \qquad X \approx u \tag{21}$$

The data in Table 3 show that, with reference to the experimental conditions, the equations in (21) allow only a very rough estimation of the variable X. On the contrary, by using Eqs. (19) and (20), the estimations of A and $X = 2(A-1)/A$ are substantially correct within the validity of the assumption made. It is useful to remember that these assumptions are:

- isothermal and isobaric system;
- anode effectively de-coupled from the cathode;
- anodic flow pattern assimilable to that of an ideal tubular reactor;
- irreversible kinetics, first order in respect to the hydrogen;
- constant mass transfer coefficient.

When X is calculated by means of Eqs. (19) and (20), the result of Fig. 3 is obtained, where the $X - Y$ trend is shown to really correspond to the linear correlation of Eq. (19); moreover, a unique straight line allows the contemporary representation of the two subseries of data, which correspond to very different composition conditions. Only one warning is necessary, that is the choice of a unique external reference condition for both the subseries, so that the constant k_a is really the same for all the data; choosing the inlet condition of the first subseries as reference it is necessary to add 34 mV to the measured voltage of the other subseries to allow for the less favourable inlet conditions. The linearity and the uniqueness of the obtained correlation are significant results. As said before, it is not possible to obtain similar results by calculating X through the oversimplified equations in (21) (see Fig. 2).

In other words, using the equations in (19), with A from Eq. (20), k_a is a known parameter, corresponding to the chosen constant current, A is a function of the utilisation factor, η is intended to be measured as a function of u. The transport coefficient k_c

must be considered as an adjustable parameter, for which the most probable estimation is derived from the data correlation. In synthesis, this is a typical identification problem. When k_c depends on flow dynamics, it can be expressed by equations like (11) in terms of Sherwood, Reynolds and Schmidt numbers; then, the best-fit operation aims to determine the correlation exponents and especially that of the Reynolds number, in which the flow pattern effects are summarised.

In the case under examination, from the slope of the linear correlation and the last equation in (19) the following simple result is obtained:

$$k_c \approx 2.1 k_a \approx 5.2 \times 10^{-2}\,\mathrm{cm\,s^{-1}} = \text{const.} \tag{22}$$

Thanks to the use of an unique external reference, Eq. (22) shows that the anodic diffusive resistances are significant, being about one half of the total, and really independent of the flow conditions.

For this last purpose, it is useful to observe that the diffusive resistances can, in general, be split into two parts; this is equivalent to assuming that the transport mechanism consists of two paths in series, the first depending only on the geometry of the condensed or still phases and independent of the flow dynamics and the second regarding the moving gaseous phase and so depending on the flow dynamics:

$$\frac{1}{k_c} = \frac{1}{k_{cCP}} + \frac{1}{k_{cG}}, \quad k_{cCP} = \text{const.}, \quad k_{cG} = f(v) \tag{23}$$

A result such as that in Eq. (22) corresponds to the statement that the anodic diffusive resistance of an Ansaldo MCFC are prevalently of the first type, while the gas phase resistances are negligible:

$$k_c \approx k_{cCP} \approx k_{cM}, \qquad k_{cG} \gg k_{cCP} \tag{24}$$

In other words, the distributing plates close to the electrodes induce a gas flow pattern which is effective in minimising the diffusive path of the reagents from the moving bulk gas to the still electrode structure.

It is remarkable that the structure of the coefficient k_{cCP} is not affected by the bulk flow leaving the anode (see Appendix E1, $\nu = 1$). This circumstance, together with a rough evaluation of the resistances in the still gas phase (plate holes, gas filled part of the porous electrode) and in the liquid phase (wet part of the porous electrode), confirms that the last are controlling.

In effect, the whole phenomenon is very articulated: the macroscopic flow fields are obviously relevant in the transport through the moving gas; the bulk flow effects should also be considered as acting with the diffusive fluxes in the transport through the still gas; the crossing of the gas–liquid interface involves the solubility of the reagents; finally, the transport through the liquid phase should not be affected by the bulk flow, as this is certainly negligible due to dilution. A slightly more analytical discussion of the bulk flow effects is reported in Appendix E1.

Allowing for the value assumed by the constant k_a in the experimental conditions considered ($k_a \approx 2.5 \times 10^{-2}\,\mathrm{cm\,s^{-1}}$), Eq. (22) leads to an estimation of the transport coefficient of the order of $k_c \approx 5 \times 10^{-2}\,\mathrm{cm\,s^{-1}}$, which is at least an order of magnitude lower than that expected for a controlling gas phase: so from this point of view a controlling liquid phase appears to be very likely.

3.2. Cathodic tests

The analysis of the cathodic diffusive resistances is more complex and, at the same time, less interesting because the effects of cathodic flow rate changes are much more moderate. This fact can be related to one or more of the following considerations.

In the first place, cathodic flow rates are decidedly greater than anodic ones, so that the flow field effects on mass transport are correspondingly less important. In the second place, there are some pertinent observations to be made on the comparison of the diffusive losses, which are independent of the flow dynamics, with the intrinsic cathodic kinetics; it is known that this kinetics depends mainly on the oxygen concentration through a fractional reaction order (for instance, 0.5–0.7 [4]) and it is certainly slower (greater activation losses) than the anodic one; both these circumstances make the diffusive effects less appreciable.

A third and probably conclusive effect regards the oxygen concentration changes during the reaction: the rather low utilisation factor (about 6%) and a decreasing flow rate act to maintain the oxygen concentration almost constant (see Appendix E2).

Therefore, while the anodic kinetics varies sensibly, the cathodic kinetics, at least under the experimental condition tested, should not vary by more than a few percentage points. The effects of the composition field on the longitudinal flow electrodes of a molten carbonate cell, the more relevant anodic ones and the much smaller cathodic ones, can be directly observed in Fig. E1.

The small voltage changes (less than 15 mV, that is about 2%) observed in the cathodic subseries were in agreement with what was just said in order of magnitude. More particularly, the non-monotonic trends, provided they are significant, could be connected to little non-uniformity in the internal temperature field, which are not completely eliminated by the thermal regulation, or, more probably, connected to coupling effects with the more sensitive anode. In other words, while the anodic perturbations can be considered well de-coupled from the cathodic behaviour, the cathodic perturbations could modify the anodic behaviour more than they modify the cathodic behaviour.

All that considered, the cathodic effects are too small and the acting phenomena too numerous and non-sufficiently controlled to risk a quantitative interpretation. On the contrary, the anodic effects are relevant and can be reliably attributed to the hydrogen concentration changes along the reaction coordinate.

3.3. Results

In short, from the above example of constant current analysis, the following conclusions can be drawn:

- The mass transport phenomena at an MCFC anode can be determined by means of perturbative methods applied to the

inlet anodic flow rate, the cathodic conditions and the cell current delivered remaining unchanged.

- The changes in the cell voltage can be directly related to the hydrogen concentration field along the anode; however, the effective mean concentration must be evaluated with some attention to the real flow conditions of the anodic gas, in agreement with chemical reactor theory fundamentals.
- The anodic analysis results indicate that the anodic diffusive resistances are significant and can be considered comparable with the anodic activation resistances.
- The mass transport phenomena and the composition field effects are much less evident at the cathode and, presumably, less important than the cathodic activation losses.
- The diffusive losses appear to be negligible in comparison to the activation losses at the cathode and comparable to the activation losses at the anode. As it is known that the activation losses at the anode are lower than those at the cathode, the concentration effects are, as a whole, responsible for a relatively small part of the total losses. However, as the anodic utilisation factor increases, these effects become more and more evident.
- The diffusive losses within the moving gas are negligible, while the ones inside the liquid appear to be controlling. This, among other considerations, demonstrates the effectiveness of the distributing plates used in the Ansaldo Fuel Cells technology.

4. An example in terms of limit currents

Tables 5 and 6 report some experimental data, in terms of limit currents, which have been obtained under constant flow rate conditions and by varying the concentration of the anodic feed. These data have already been presented in a previous work [5], where a substantial proportionality between the limit current and the inlet hydrogen molar fraction (y_{Ao}) was demonstrated. Those conclusions are now more precisely discussed.

In agreement with what has been discussed in the previous section and allowing for the same assumptions on a longitudinal flow anode, the relationship between the limit current (that is k_L), the transport coefficient k_c and the inlet composition y_{Ao} should be expressed by

$$\frac{k_c}{k_f} = -y_{Ao}u_L - (1 + y_{Ao})\ln(1 - u_L),$$

$$u_L = \frac{k_L}{k_f} = \frac{J_L}{nFy_{Ao}k_f} \tag{25}$$

Assuming that k_c and k_f are constant, Eq. (25) can be written in the form

$$J_L = \frac{nFk_c y_{Ao}}{A_L} = \frac{\text{const.}\ y_{Ao}}{A_L},$$

$$\frac{1}{A_L} = \left[-y_{Ao} - (1 + y_{Ao})\ln\frac{1 - u_L}{u_L}\right] \tag{26}$$

in which the simple proportionality between J_L and y_{Ao} is corrected in order to allow for the non-uniform concentration field.

Table 5
Ansaldo Fuel Cells: test condition

Central point	
Anodic flow rates [mol s^{-1} × 10^5]	
H_2	6.5[a]
CO_2	1.4
N_2	15.8[a]
H_2O	2.3
Total	26.0
Cathodic flow rates [N m^3 h^{-1} × 10^3]	
O_2	15.1
CO_2	14.3
N_2	125.0
Total	154.4
Cell current	Limit current
Flow rates	Constant flow rates
Hydrogen mol fraction	$0.06 < y_{Ao} < 0.70$

[a] H_2 and N_2 flow rates are changed in a complementary way, so that the total anodic flow rate is kept constant.

Table 6
Ansaldo Fuel Cells: limit current results

y_{Ao}	J_L [mA cm^{-2}]	u_L	A_L[a]	y_{Ao}/A_L
0.699	270	0.422	1.510	0.463
0.583	260	0.487	1.588	0.367
0.437	230	0.575	1.700	0.257
0.350	205	0.640	1.804	0.194
0.291	178	0.668	1.842	0.158
0.250	153	0.669	1.812	0.138
0.219	140	0.699	1.872	0.117
0.194	120	0.676	1.796	0.108
0.175	100	0.624	1.667	0.105
0.146	100	0.748	1.972	0.074
0.117	80	0.747	1.950	0.060
0.097	68	0.766	1.980	0.049
0.087	55	0.690	1.761	0.049
0.079	55	0.761	1.950	0.041
0.070	50	0.781	2.010	0.035
0.062	40	0.705	1.777	0.035

[a] $A_L = [-y_{Ao} - (1 + y_{Ao})\ln(1 - u_L)/u_L]^{-1}$.

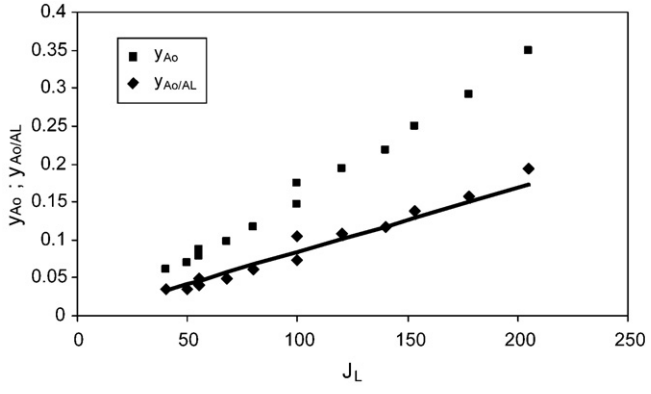

Fig. 4. Effects of the inlet hydrogen mol fraction y_{Ao} and of the mean hydrogen mol fraction y_{Ao}/A_L on the limit current.

Only in the case of very low utilisation factors can it be assumed that the corrective term A_L connected to the concentration field is equal unity (uniform concentration) and can J_L be considered directly proportional to y_{Ao}. In Fig. 4, the differences between the two correlation methods are shown: on the one hand, both the $J_L - y_{Ao}$ and the $J_L - y_{Ao}/A_L$ correlations indicate straight lines from the origin of the axes, but the two slopes are completely different. In other words, neglecting the factor A_L results in a serious underestimation of the transport coefficient k_c.

5. Conclusions

As concluded in Part 1 of this work, the analysis of the diffusive resistance in a finite-size electrode can lead to a non-linear problem at the laboratory scale, where temperature and voltage can be assumed uniform on the cell plane. At least two interlinked factors have to be considered:

- the local diffusive resistances set and
- the concentration distribution on the electrode.

The first can be determined only after estimating the second by means of an adequate physical–mathematical description. To do this it is particularly useful to refer to a close analogy between electrode kinetics and heterogeneous chemical kinetics with the reaction at the boundary and to use this analogy within the chemical reactor theory.

This kind of analysis can be successfully applied to experimental fuel cell data. The consideration of data from Ansaldo MCFCs makes it possible to say that

- the diffusive resistance at the cathode has less relevant effects, while
- the anodic resistances are comparable with the activation ones and
- are independent of the inlet flow rate, that is
- prevailingly localised in the liquid phase;
- a superficial analysis of the concentration field effects, in terms of constant current and limit current, can lead to a gross overestimation of the mass transport coefficients.

Acknowledgement

The authors wish to thank Ansaldo Fuel Cells for the data placed at their disposal and for its generous help during this work.

Appendix D. Comparison of electrodes

The reference to limit models, or ideal reactors, and their comparison are fundamental classical arguments of the chemical reactor theory. In terms of continuous systems, in particular, two ideal reactors are compared, the continuous stirred tank reactor (CSTR) and the plug flow reactor (PFR). The undoubted usefulness of these methodological schemes in the chemical reactor analysis, both homogeneous and heterogeneous, suggests that they should be more frequently utilised in electrochemical reactor analysis too. In Part 1, Appendix C, the behaviour of the "mixed", that is the CSTR-like, and the "longitudinal flow", that is the PFR-like, electrodes have been discussed, especially with reference to their characteristics as complex electrodes; here further remarks will be made to clarify their differences from the electrochemical point of view.

A comparison of the PFR and CSTR, when strictly considered as chemical reactors, highlights, as known, the superiority of the first, which presents a greater mean reaction rate. When dealing with electrodes, the comparison can be better appreciated if it is made in terms of voltage, the utilisation factors (that is the currents or the mean reaction velocities), the active surfaces per unit flow rate and the mass transfer resistances being the same. Then, for the two reactors, or electrodes, equal flow dynamic constant k_f, transport constant k_c (or at least their ratio) and the utilisation factor u are assumed.

A first difference in favour of the longitudinal flow reactor regards the limit utilisation factors, which are, for the two cases, respectively

$$\begin{aligned} &\text{PFR} \quad u_L = 1 - \exp\left(-\frac{k_c}{k_f}\right) \\ &\text{CSTR} \quad u_L = \frac{1}{1 + (k_f/k_c)} \end{aligned} \tag{D1}$$

the first being greater than the second: the comparison at equal u cannot be extended to the range of higher values only accessible to the PFR.

In the range where the comparison is possible, it is

$$u = 1 - \exp\left(-\frac{K}{k_f}\right) = \frac{1}{1 + (k_f/K)}, \qquad \frac{1}{K} = \frac{1}{k_o} + \frac{1}{k_c} \tag{D2}$$

or

$$\begin{aligned} &\text{PFR} \quad \frac{k_f}{k_o} = -\frac{1}{\ln(1-u)} - \frac{k_f}{k_c} \\ &\text{CSTR} \quad \frac{k_f}{k_o} = \frac{1-u}{u} - \frac{k_f}{k_c} \end{aligned} \tag{D3}$$

At equal k_f/k_c and u, the longitudinal flow, thanks to a better concentration distribution, requires a lower intrinsic kinetic constant k_o, which means lower activation losses. The logarithm of the ratio of the two k_o values can be directly connected to the differences between the activation losses of the two electrodes

$$\beta\,\Delta\eta = \ln\left[-\frac{1}{\ln(1-u)} - \frac{k_f}{k_c}\right] - \ln\left[\frac{1-u}{u} - \frac{k_f}{k_c}\right], \qquad u < \frac{1}{1 + (k_f/k_c)} \tag{D4}$$

The trend of this difference, which tends to diverge when the mixed electrode is approaching its limit current condition, is reported in Fig. D1 for different values of the coefficient ratio k_f/k_c.

From another anymore relevant point of view, at least here, the comparison of electrodes presenting different flow characteristics involves the interpretation of the experimental data and, in particular, affects the analysis of the diffusive resistances: the

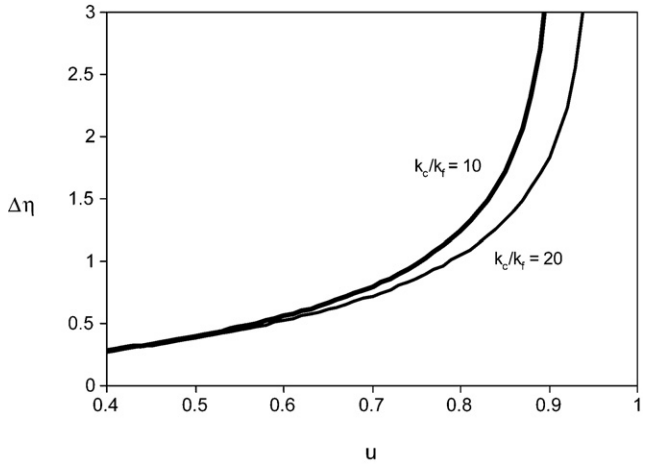

Fig. D1. Comparison of a longitudinal flow electrode (PFR) and a mixed electrode (CSTR) in terms of voltage losses as a function of the utilisation factor and for different values of k_c/k_f. The difference $\Delta\eta$ between the CSTR losses and the PFR ones is reported: each unity on the ordinate scale corresponds to about 40 mV ($k_c/k_f = 20$, $u_{LCSTR} = 0.95$; $k_c/k_f = 10$, $u_{LCSTR} = 0.91$).

characterisation of one electrode in terms of exchange current and limit current does not allow a univocal estimation of the transport coefficient, unless the electrode is a simple one. In the simple cases it is straightforwardly

$$\frac{1}{k_o} = \frac{1}{k_a} - \frac{1}{k_L}, \qquad k_c = k_L \tag{D5}$$

and the transport coefficient is directly connected to the limit current.

A continuous mixed electrode (CSTR) with given exchange and limit currents behaves just like simple electrode (see Fig. D2)

$$\frac{1}{k_o} = \frac{1}{k_a} - \frac{1}{k_L}, \qquad \frac{1}{k_c} = \frac{1}{k_L} - \frac{1}{k_f} \tag{D6}$$

but its limit current also depends on the flow constant k_f and, inversely, the limit current is not directly interpretable in terms of a transport coefficient.

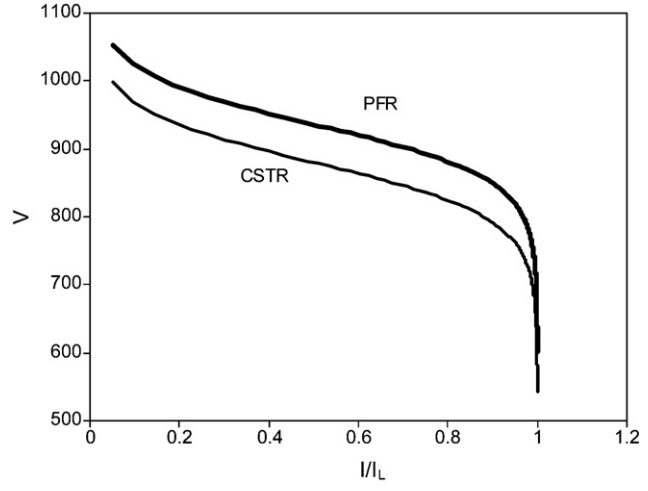

Fig. D2. A comparison of the electrodes in terms of voltage at different currents, the exchange and the limit current being unchanged. The electrode voltage reported is in mV.

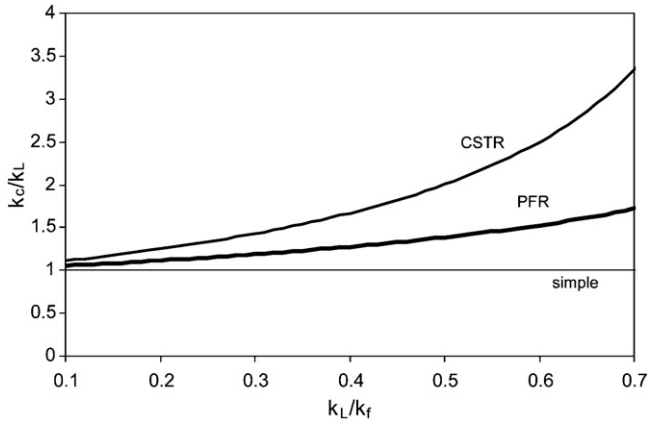

Fig. D3. Comparison of electrodes in the identification problem: the estimation of the transport coefficient at equal exchange and limit currents.

The longitudinal flow electrode (PFR), at equal exchange and limit current, also shows qualitatively similar performances (see Fig. D2)

$$\frac{1}{k_o} = -\frac{1}{k_f \ln(1-(k_a/k_f))} + \frac{1}{k_f \ln(1-(k_L/k_f))},$$
$$k_c = -k_f \ln\left(1 - \frac{k_L}{k_f}\right) \tag{D7}$$

and the limit current is again affected by the flow constant, but in a different manner from the mixed electrode and with a low current behaviour which risks being attributed to a different exchange current.

As an example, in Fig. D3 the ratio k_c/k_L between the transport coefficient and limit coefficient of the three electrodes considered (simple, CSTR, PFR) are reported as functions of the ratio k_L/k_f between the limit and flow coefficients. It is quite evident that the identification of a transport coefficient may be completely misinterpreted if these flow effects are not correctly taken into account.

Appendix E. Bulk flow effects

In fuel cell electrodes the electrochemical reactions are usually unbalanced in terms of mol numbers and in terms of mass. This fact might add significant non-linearity effects to the local kinetics as well as to the concentration distribution on the cell.

E1. Local effects

As is well known, the molar fluxes of the reagents from the bulk gas to the electrode surface and those of the products in the opposite direction contain two terms. The first, of diffusive nature, can be expressed through the Fick equation, while the second is a bulk flow term, which is due to the mean molar velocity of the fluid, that is the total flux, the sum of all component fluxes:

$$N_i = N_T y_i - C_T D_A \left(\frac{dy_A}{dz}\right), \quad N_T = \sum N_i \tag{E1}$$

On the other hand, the reaction stoichiometry states that $N_i = \nu_i N_A/\nu_A$, so, for the key reagent migrating towards the electrode, Eq. (E1) can be written

$$N_A = -C_T D_A \left(\frac{dy_A/dz}{1+\nu y_A}\right), \quad \nu = -\frac{\sum \nu_i}{\nu_A} \tag{E2}$$

and, by integrating on a thickness s between y_{A1} and y_{A2}, the flux expression is obtained

$$N_A = \ln\left[\frac{1+\nu y_{A1}}{1+\nu y_{A2}}\right]\left(\frac{C_T D_A}{\nu s}\right) \approx (y_{A1}-y_{A2}) \times \left(\frac{C_T D_A}{s}\right)\left[1-\frac{\nu(y_{A1}+y_{A2})}{2}\right] \tag{E3}$$

which is non-linear in the composition difference. When $\nu \neq 0$, the bulk flow effect is negligible only for very dilute solutions. Table E1 reports the values for ν for MCFC, PEMFC and SOFC electrodes. For $\nu > 0$ the bulk flow contrasts with the motion towards the electrode, so that the key reagent has a flux lower than the one associated with a simple diffusive path ($\nu = 0$); for $\nu < 0$ the effects are the opposite.

For molten carbonate fuel cells and, in particular, under the experimental conditions reported in Tables 1 and 2, these local effects, especially the anodic ones, should be present and appreciable. If, on the contrary, similar effects have not been detected, a likely interpretation could be found in the role of the liquid phase. If two phases, gas and liquid, are considered, their separation interface can be assumed to be close to equilibrium

$$y_{Ai} = m_A x_{Ai} \tag{E4}$$

Moreover, the molar flux of the key reagent is the same in each phase

$$N_A = (y_A - y_{Ai})\left(\frac{C_G D_{AG}}{s_G}\right) f_G, \quad f_G = \left[1-\frac{\nu(y_A+y_{Ai})}{2}\right] \tag{E5}$$

$$N_A = (x_{Ai} - x_{As})\left(\frac{C_{LP} D_{ALP}}{s_L}\right) f_{LP}, \quad f_{LP} = \left[1-\frac{\nu(x_{Ai}+x_{As})}{2}\right] \tag{E6}$$

and equal to the reaction rate per unit surface

$$N_A = k C_{LP} x_{As} \tag{E7}$$

Under such conditions, the transport phenomena are controlled by one or the other phase, according to the value assumed by the ratio

$$\frac{m_A f_G C_G D_{AG}/s_G}{f_{LP} C_{LP} D_{ALP}/s_{LP}} \tag{E8}$$

As the gaseous species A has low solubility ($m_A \gg 1$) and $C_G D_{AG} > C_{LP} D_{ALP}$, comparable resistances in the two phases require a liquid thickness much lower than the gas one (for instance, $s_L < 10^{-4} s_G$), so that it is quite probable that the liquid is the controlling phase. In this case, as $y_{Ai} = m_A x_{Ai} \approx y_A$ and putting $y_{As} = m_A x_{As}$, the flux is

$$N_A \approx (y_A - y_{As})\left(\frac{C_{LP} D_{ALP}}{m_A s_{LP}}\right) f_{LP} \tag{E9}$$

where the global transport coefficient

$$k_c \approx \frac{C_{LP} D_{ALP}}{m_A s_{LP}} \tag{E10}$$

depends on the transport properties and geometry of the controlling phase and on the solubility coefficient m_A, while the bulk flow effects become quite negligible because of the high dilution of A in the liquid phase

$$x_{Ai}, x_{As} \ll 1, \qquad f_{LP} \approx 1 \tag{E11}$$

Therefore, the absence of evident bulk flow effects in local diffusive phenomena is not surprising; on the contrary, this fact can be considered as a strong indication in favour of the liquid controlling assumption.

E2. Effects on the composition field

The molar fluxes unbalance shows a more appreciable effect on the composition of the bulk gas flowing on the electrode. By expressing the molar flow rates of the various components as well as the total molar flow rate in terms of the utilisation factor,

$$F_i = F_{io} - \frac{F_{Ao} u \nu_i}{\nu_A}, \qquad F_T = F_{To} + F_{Ao} u \nu \tag{E12}$$

Table E1
Molar and mass unbalance for electrode reactions

Electrode	In	Out	A	$\nu = -\sum \nu_i/\nu_A$	$\nu_m = -\sum \nu_i M_i/\nu_A M_A$
MCFC					
Anode	H_2	CO_2, H_2O	H_2	1	30
Cathode	$2CO_2$, O_2	–	O_2	−3	−3.75
Cathode	$2CO_2$, O_2	–	CO_2	−1.5	−1.87
PEMFC					
Anode	H_2	–	H_2	−1	−1
Cathode	O_2	$2H_2O$	O_2	1	0.125
SOFC					
Anode	H_2	H_2O	H_2	0	8
Cathode	O_2	–	O_2	−1	−1

the molar fraction of the key reagent is

$$y_A = y_{Ao}\left(\frac{1-u}{1+\nu y_{Ao}u}\right) \tag{E13}$$

and the dependence on the molar unbalance is evident.

In general, the dependence of kinetics on the key concentration can be expressed in terms of an apparent order γ

$$N_A = r = k_o C_T y_{As}^{\alpha} = k_o C_T y_A^{\gamma}, \quad 0<\alpha<1, \quad \alpha<\gamma<1 \tag{E14}$$

which, in comparison with the true order α, summarises the importance of the transport phenomena ($\gamma=\alpha$ for kinetics controlling; $\gamma=1$ for transport controlling). By combining Eqs. (E13) and (E14) the dependence of the kinetics on the bulk gas composition (y_{Ao}) becomes

$$r = k_o C_T\left[\frac{y_{Ao}(1-u)}{1+\nu y_{Ao}u}\right]^{\gamma} \approx k_o C_T (y_{Ao})^{\gamma}[1-\gamma(1+\nu y_{Ao})u] \tag{E15}$$

$$-\left(\frac{1}{r}\right)\left(\frac{dr}{du}\right)_{u=0} \approx \gamma(1+\nu y_{Ao}) \tag{E16}$$

For an MCFC the effect is much more important at the anode ($\nu=1$ and, with reference to Tables 1 and 2, $y_{Ao}=0.2$–0.8, $u<0.3$), where the corrective term on the right hand side of Eq. (E15) leads to reaction rate variations up to 60% in comparison to the initial values; the effect is much slighter at the cathode ($\nu=-3$, $y_{Ao}\approx 0.16$, $u\approx 0.06$), where the decreasing flow rate contributes to maintaining the reaction rate substantially unchanged, with differences of less than about 3% of the initial value.

The corrections to the local kinetics (Eq. (E15)) due to the unbalancing parameter $\nu\neq 0$ also obviously affect the averaging operations and the values obtained for the parameter A, as defined by Eq. (5). For instance, in those cases where linear kinetics ($\alpha=\gamma=1$) and a longitudinal flow can be assumed, the differential balance equation along the adimensional axial coordinate ζ

$$k_f\frac{du'}{d\zeta} = \frac{K(1-u')}{1+\nu y_{Ao}u'}, \quad \zeta=0, \quad u'=0, \quad \zeta=1, \quad u'=u \tag{E17}$$

leads to the integral

$$\frac{K}{k_f} = -\nu y_{Ao}u - (1+\nu y_{Ao})\ln(1-u), \qquad k_a = k_f u,$$
$$A = \frac{K}{k_a} \tag{E18}$$

and, finally to

$$A = -\nu y_{Ao} - (1+\nu y_{Ao})\frac{\ln(1-u)}{u} \tag{E19}$$

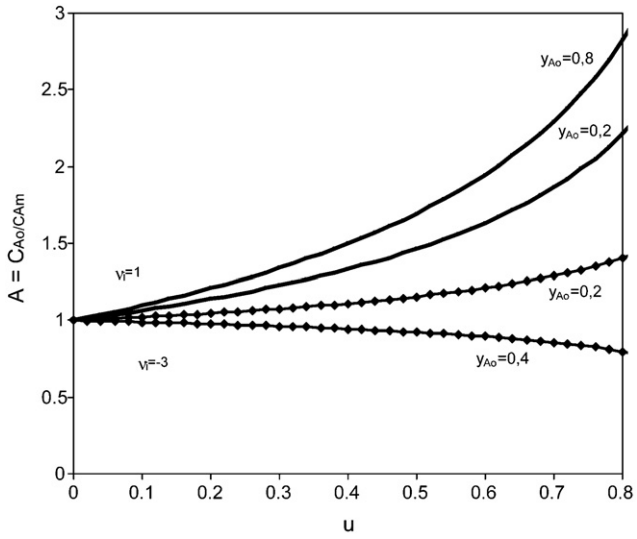

Fig. E1. Effects if the inlet composition and the flow rate changes on the MCFC longitudinal flow (PFR) electrodes (anode: $\nu=1$; cathode: $\nu=-3$).

This equation, with $\nu=1$ is the one used in Sections 3 and 4 for an MCFC anode. For a very diluted system as well as for balanced reactions ($\nu=0$) the same Eq. (E19) becomes

$$y_{Ao}\to 0, \quad A \approx -\left(\frac{1}{u}\right)\ln(1-u) \tag{E20}$$

which is the one used in Part 1, Appendix C for describing the longitudinal constant flow electrode. Moreover, for very low utilisation factors, Eq. (E19) can be rewritten as

$$u\to 0, \quad A \approx 1+(1+\nu y_{Ao})\frac{u}{2} \tag{E21}$$

while the equality of A with the mean utilisation

$$\nu y_{Ao}\to 0, \quad u\to 0, \quad A\approx 1+\frac{u}{2} \tag{E22}$$

is correct only when both ν, y_{Ao} and u are very small.

The effects of the molar unbalance on the averaging coefficient A of the two longitudinal flow electrodes of an MCFC are reported in Fig. E1. The greater relevance of the anodic effect is evident. The cathodic effect is much smaller and may even change its sign at an increase in the oxygen content ($y_{Ao}>0.33$).

In practice, the unbalance effects in MCFC are even lower than those of Fig. E1 because an intrinsic kinetics where O_2 is the key reagent ($\nu=-3$) interacts with transport phenomena where CO_2 is likely to be controlling ($\nu=-1.5$).

References

[1] P. Costa, B. Bosio, J. Power Sources 172 (2007) 334–345.
[2] J.O.M. Bockris, S. Srinivasan, Fuel Cells: Their Electrochemistry, McGraw-Hill, New York, 1969.
[3] B. Bosio, P. Capobianco, E. Arato, Adv. Sci. Technol. 29 (2000) 1277–1284.
[4] B. Bosio, P. Costamagna, F. Parodi, Chem. Eng. Sci. 54 (1999) 2907–2916.
[5] E. Arato, B. Bosio, P. Costa, F. Parodi, J. Power Sources 102 (2001) 74–81.